J|A|C|S ARTICLES

Published on Web 09/23/2010

Stepwise Assembly of Coordination-Based Metal−Organic Networks

Revital Kaminker,[†] Leila Motiei,[†] Antonino Gulino,[§] Ignazio Fragalà,[§] Linda J. W. Shimon,[‡] Guennadi Evmenenko,[¶] Pulak Dutta,[¶] Mark A. Iron,[‡] and Milko E. van der Boom*,[†]

Departments of Organic Chemistry and Chemical Research Support, Weizmann Institute of Science, Rehovot 76100, Israel, Dipartimento di Scienze Chimiche, Università di Catania, Catania 95125, Italy, and Department of Physics and Astronomy, Northwestern University, Evanston, Illinois 60208-3113

Received June 23, 2010; E-mail: milko.vanderboom@weizmann.ac.il

Abstract: Metal−organic networks (MONs) were created by a stepwise solution deposition approach from vinylpyridine-based building blocks and $PdCl_2$. The combined experimental and computational study demonstrates the formation of saturated, structurally organized systems on solid supports. The rigid nature and geometry of the components are well-suited to form honeycomb and parallelogram structures, as predicted by a computational study. Detailed structural information of the new MONs was obtained by optical (UV/vis) spectroscopy, ellipsometry, atomic force microscopy (AFM), X-ray photoelectron spectroscopy (XPS), and synchrotron X-ray reflectivity (XRR). Notably, the XPS elemental composition indicates the formation of a palladium coordination-based network.

Introduction

Selective metal−ligand coordination is a powerful synthon for the assembly of supramolecular structures in solution and in the solid-state.[1−6] Numerous interesting systems have been reported, and a strong fundamental basis has been developed to guide the formation of hybrid materials. These materials include metal−organic polymers, networks, frameworks, grids, and clusters.[2] In particular, highly porous metal−organic frameworks (MOFs) have attracted much attention[3] partially due to the prospect of large-scale industrial use for the storage of gases. Wöll and Fischer demonstrated very recently that a stepwise build-up of MOFs results in a high level of control over the structure of these crystalline materials.[4] Studies on layer-by-layer growth using metal−ligand coordination appeared already in the literature during the early 1990s and include the works of Li, Swanson, Mallouk, and Ulman.[5] Nevertheless, it is still a tremendous challenge to *a priori* design ordered surface-confined MOFs and metal−organic networks (MONs) based on a given molecular structure.[4,6]

Sagiv's layer-by-layer deposition methodology with the aim of generating well-defined molecular aggregates at interfaces has proven useful for the generation of a wide variety of

[†] Department of Organic Chemistry, Weizmann Institute of Science.
[§] Dipartimento di Scienze Chimiche, Università di Catania.
[‡] Department of Chemical Research Support, Weizmann Institute of Science.
[¶] Department of Physics and Astronomy, Northwestern University.

(1) (a) Marschall, M.; Reichert, J.; Weber-Bargioni, A.; Seufert, K.; Auwärter, W.; Klyatskaya, S.; Zoppellaro, G.; Ruben, M.; Barth, J. V. *Nature Chem.* **2010**, *2*, 131. (b) Chen, T.; Pan, G.-B.; Wettach, H.; Fritzsche, M.; Hger, S.; Wan, L.-J.; Yang, H.-B.; Northrop, B. H.; Stang, P. J. *J. Am. Chem. Soc.* **2010**, *132*, 1328. (c) Mal, P.; Breiner, B.; Rissanen, K.; Nitschke, J. R. *Science* **2009**, *324*, 1697. (d) Golubkov, G.; Weissman, H.; Shirman, E.; Wolf, S. G.; Pinkas, I.; Rybtchinski, B. *Angew. Chem., Int. Ed.* **2009**, *48*, 926. (e) Oliveri, C. G.; Ulmann, P. A.; Wiester, M. J.; Mirkin, C. A. *Acc. Chem. Res.* **2008**, *41*, 1618. (f) South, C. R.; Piñón, V., III; Weck, M. *Angew. Chem., Int. Ed.* **2008**, *47*, 1425. (g) Ruben, M.; Rojo, J.; Romero-Salguero, F. J.; Uppadine, L. H.; Lehn, J.-M. *Angew. Chem., Int. Ed.* **2004**, *43*, 3644.

(2) (a) Eberle, F.; Saitner, M.; Boyen, H.-G.; Kucera, J.; Gross, A.; Romanyuk, A.; Oelhafen, P.; D'Olieslaeger, M.; Manolova, M.; Kolb, D. M. *Angew. Chem., Int. Ed.* **2010**, *49*, 341. (b) Greenstein, M.; Ben Ishay, R.; Maoz, B. M.; Leader, H.; Vaskevich, A.; Rubinstein, I. *Langmuir* **2010**, *26*, 7277. (c) Tuccitto, N.; Delfanti, I.; Torrisi, V.; Scandola, F.; Chiorboli, C.; Stepanenko, V.; Würthner, F.; Licciardello, A. *Phys. Chem. Chem. Phys.* **2009**, *11*, 4033. (d) Nishimori, Y.; Kanaizuka, K.; Kurita, T.; Nagatsu, T.; Segawa, Y.; Toshimitsu, F.; Muratsugu, S.; Utsuno, M.; Kume, S.; Murata, M.; Nishihara, H. *Chem. Asian J.* **2009**, *4*, 1361. (e) Johannes, A. A. W. E.; Shengbin, L.; Steven, D. F. *Angew. Chem., Int. Ed.* **2009**, *48*, 7298. (f) George, S. M.; Yoon, B.; Dameron, A. A. *Acc. Chem. Res.* **2009**, *42*, 498. (g) Fischer, R. A.; Wöll, C. *Angew. Chem., Int. Ed.* **2009**, *48*, 6205. (h) Kanaizuka, K.; Haruki, R.; Sakata, O.; Yoshimoto, M.; Akita, Y.; Kitagawa, H. *J. Am. Chem. Soc.* **2008**, *130*, 15778. (i) Maspoch, D.; Ruiz-Molina, D.; Veciana, J. *Chem. Soc. Rev.* **2007**, *36*, 770.

(3) (a) Farha, O. K.; Malliakas, C. D.; Kanatzidis, M. G.; Hupp, J. T. *J. Am. Chem. Soc.* **2010**, *132*, 950. (b) Deng, H.; Doonan, C. J.; Furukawa, H.; Ferreira, R. B.; Towne, J.; Knobler, C. B.; Wang, B.; Yaghi, O. M. *Science* **2010**, *327*, 846. (c) Makiura, R.; Motoyama, S.; Umemura, Y.; Yamanaka, H.; Sakata, O.; Kitagawa, H. *Nat. Mater.* **2010**, *9*, 565. (d) Ma, L. Q.; Lin, W. *Angew. Chem., Int. Ed.* **2009**, *48*, 3637. (e) Long, R.; Yaghi, O. M. *Chem. Soc. Rev.* **2009**, *38*, 1213. (f) Furukawa, H.; Yaghi, O. M. *J. Am. Chem. Soc.* **2009**, *25*, 8876. (g) Murray, L. J.; Dinca, M.; Long, J. R. *Chem. Soc. Rev.* **2009**, *38*, 1294. (h) Ma, L. Q.; Mihalcik, D. J.; Lin, W. B. *J. Am. Chem. Soc.* **2009**, *131*, 4610. (i) Yaghi, O. M.; O'Keeffe, M.; Ockwig, N. W.; Chae, H. K.; Eddaoudi, M.; Kim, J. *Nature* **2003**, *423*, 705.

(4) (a) Shekhah, O.; Wang, H.; Paradinas, M.; Ocal, C.; Schupbach, B.; Terfort, A.; Zacher, D.; Fischer, R. A.; Wöll, C. *Nat. Mater.* **2009**, *8*, 481. (b) Shekhah, O.; Wang, H.; Zacher, D.; Fischer, R. A.; Wöll, C. *Angew. Chem., Int. Ed.* **2009**, *48*, 5038. (c) Shekhah, O.; Wang, H.; Kowarik, S.; Schreiber, F.; Paulus, M.; Tolan, M.; Sternemann, C.; Evers, F.; Zacher, D.; Fischer, R. A.; Wöll, C. *J. Am. Chem. Soc.* **2007**, *129*, 15118.

 10.1021/ja105518n © **2010 American Chemical Society**

"dressed" and functional surfaces.[7−18] Prominent examples of thin films include Decher's alternating deposition of polyelectrolytes,[9] Marks's noncentrosymmetric materials,[10] and the Hf- and Zr-complexation chemistry of Mallouk, Katz, and of Shanzer and Rubinstein.[11] Some of these materials have been used to fabricate devices,[12,13] including (i) solar cells, (ii) organic light emitting diodes (OLEDs), (iii) organic field-effect transistors (OFETs), and (iv) electro-optic modulators.

Stepwise deposition of metal−organic structures often involves systems in which the molecular components are coordinatively connected in the direction of the film growth, resulting in the formation of chainlike structures.[14−16] Lateral ordering can be induced by, for instance, the use of $\pi-\pi$ interactions.[17,18] Molecular components having multiple metal-binding sites for platinum group metals to generate complex architectures in solution have been thoroughly explored.[19] However, the use of similar systems to generate metal−organic structures on solid supports via a stepwise solution-based deposition approach is rare.[16] MONs can be designed by satisfying the following requirements: (i) each of the organic components should bind to three or more metal centers, (ii) two or more organic components should coordinate to the same metal center, (iii) at least one of the above should be a nonlinear structure.

Herein, we demonstrate the assembly of surface-confined coordination-based MONs. Multiple connections between organic chromophores are formed through coordination bonds between vinylpyridine groups and palladium(II) dichloride. This metal−ligand combination is structurally well-defined as it generates square-planar structures with two mutually *trans*-vinylpyridine groups. This coordination chemistry is a particular useful synthon for the induction of long-range order. Semiempirical (PM6)[20] calculations were used to select two chromophores that have the structural requirements necessary to form MONs. The new materials are generated on organic template layers covalently attached to silicon-oxide-terminated surfaces using our iterative wet-chemical deposition approach.[14] This versatile method has resulted very recently in the formation of surface-bound coordination-based oligomers,[14] fluorinated oligomers,[15] positive constructs,[16] three-dimensional (3D) ordered assemblies,[17] and exponentially growing electrochromic structures.[21,22] These latter self-propagating films have been used for the generation of electrical, addressable, multistate volatile memory with flip−flop and flip−flap−flop logic circuits and efficient inverted bulk-heterojunction solar cells.[12] Detailed structural information of the new MONs was obtained by optical (UV/vis) spectroscopy, ellipsometry, atomic force microscopy (AFM), X-ray photoelectron spectroscopy (XPS), and synchrotron X-ray reflectivity (XRR). A combination of such methods is necessary to make realistic structural assignments. Linear growth versus the number of deposition cycles (chromophore

(5) (a) Bell, C. M.; Arendt, M. F.; Gomez, L.; Schmeh, R. H.; Mallouk, T. E. *J. Am. Chem. Soc.* **1994**, *116*, 8314. (b) Bell, C. M.; Keller, S. W.; Lynch, V. M.; Mallouk, T. E. *Mater. Chem. Phys.* **1993**, *35*, 225. (c) Li, D.-Q.; Smith, D. C.; Swanson, B. I.; Farr, J. D.; Paffett, M. T.; Hawley, M. E. *Chem. Mater.* **1992**, *4*, 1047. (d) Evans, S. D.; Ulman, A.; Goppert-Berarducci, K. E.; Gerenser, L. J. *J. Am. Chem. Soc.* **1991**, *113*, 5866.

(6) (a) Makiura, R.; Kitagawa, H. *Eur. J. Inorg. Chem.* **2010**, 3715. (b) For a discussion regarding the nomenclature, see: Biradha, K.; Ramana, A.; Vittal, J. J. *Cryst. Growth Des.* **2009**, *9*, 2969.

(7) (a) Zeira, A.; Chowdhury, D.; Hoeppener, S.; Liu, S.; Berson, J.; Cohen, S. R.; Maoz, R.; Sagiv, J. *Langmuir* **2009**, *25*, 13984. (b) Wen, K.; Maoz, R.; Cohen, H.; Sagiv, J.; Gibaud, A.; Desert, A.; Ocko, B. M. *ACS Nano* **2008**, *2*, 579. (c) Ulman, A. *Chem. Rev.* **1996**, *96*, 1533. Tillman, N.; Ulman, A.; Penner, T. L. *Langmuir* **1989**, *6*, 101. (d) Netzer, L.; Sagiv, J. *J. Am. Chem. Soc.* **1983**, *105*, 674. (e) Netzer, L.; Iscovici, R.; Sagiv, J. *Mol. Cryst. Liq. Cryst.* **1983**, *93*, 415.

(8) For recent examples and reviews, see: (a) Kurita, T.; Nishimori, Y.; Toshimitsu, F.; Muratsugu, S.; Kume, S.; Nishihara, H. *J. Am. Chem. Soc.* **2010**, *132*, 4524. (b) Pan, Y.; Tong, B.; Shi, J.; Zhao, W.; Shen, J.; Zhi, J.; Dong, Y. *J. Phys. Chem. C* **2010**, *114*, 8040. (c) Eberle, F.; Saitner, M.; Boyen, H.-G.; Kucera, J.; Gross, A.; Romanyuk, A.; Oelhafen, P.; D'Olieslaeger, M.; Manolova, M.; Kolb, D. M. *Angew. Chem., Int. Ed.* **2010**, *49*, 341. (d) Tuccitto, N.; Ferri, V.; Cavazzini, M.; Quici, S.; Zhavnerko, G.; Licciardello, A.; Rampi, M. A. *Nat. Mater.* **2009**, *8*, 41. (e) Kanaizuka, K.; Haruki, R.; Sakata, O.; Yoshimoto, M.; Akita, Y.; Kitagawa, H. *J. Am. Chem. Soc.* **2008**, *130*, 15778. (f) Nishihara, H.; Kanaizuka, K.; Nishimori, Y.; Yamanoi, Y. *Coord. Chem. Rev.* **2007**, *251*, 2674. (g) Ariga, K.; Hill, J. P.; Ji, Q. *Phys. Chem. Chem. Phys.* **2007**, *9*, 2319. (h) Srinivasan, C.; Hohman, J. N.; Anderson, M. E.; Zhang, P.; Weiss, P. S.; Horn, M. W. *Proc. SPIE-Int. Soc. Opt. Eng.* **2007**, 65171I/1. (i) Onclin, S.; Ravoo, B. J.; Reinhoudt, D. N. *Angew. Chem., Int. Ed.* **2005**, *44*, 6282.

(9) (a) Cini, N.; Tulun, T.; Decher, G.; Ball, V. *J. Am. Chem. Soc.* **2010**, *132*, 8264. (b) Decher, G., Schlenoff, J. B., Eds. *Multilayer Thin Films*; Wiley-VCH: Weinheim, Germany, 2003.

(10) (a) DiBenedetto, S. A.; Facchetti, A.; Ratner, M. A.; Marks, T. J. *J. Am. Chem. Soc.* **2009**, *131*, 7158. (b) van der Boom, M. E.; Richter, A. G.; Malinsky, J. E.; Lee, P. A.; Armstrong, N. R.; Dutta, P.; Marks, T. J. *Chem. Mater.* **2001**, *13*, 15. (c) Yitzchaik, S.; Marks, T. J. *Acc. Chem. Res.* **1996**, *29*, 197. (d) Lin, W.; Lin, W.; Wong, G. K.; Marks, T. J. *J. Am. Chem. Soc.* **1996**, *118*, 8034. (e) Li, D.-Q.; Ratner, M. A.; Marks, T. J.; Zhang, C.-H.; Yang, J.; Wong, G. K. *J. Am. Chem. Soc.* **1990**, *112*, 7389.

(11) (a) Moav, T.; Hatzor, A.; Cohen, H.; Libman, J.; Rubinstein, I.; Shanzer, A. *Chem.−Eur. J.* **1998**, *4*, 502. (b) Hatzor, A.; Moav, T.; Cohen, H.; Matlis, S.; Libman, J.; Vaskevich, A.; Shanzer, A.; Rubinstein, I. *J. Am. Chem. Soc.* **1998**, *120*, 1346. (c) Mallouk, T. E.; Gavin, J. A. *Acc. Chem. Res.* **1998**, *31*, 209. (d) Keller, S. W.; Kim, H.-N.; Mallouk, T. E. *J. Am. Chem. Soc.* **1994**, *116*, 8817. (e) Katz, H. E.; Scheller, G.; Putvinski, T. M.; Schilling, M. L.; Wilson, W. L.; Chidsey, C. E. D. *Science* **1991**, *254*, 1485. (f) Haiwon, L.; Kepley, L. J.; Hong, H. G.; Akhter, S.; Mallouk, T. E. *J. Phys. Chem.* **1988**, *92*, 2597. (g) Lee, H.; Kepley, L. J.; Hong, H. G.; Mallouk, T. E. *J. Am. Chem. Soc.* **1988**, *110*, 618.

(12) (a) Motiei, L.; Yao, Y.; Choudhury, J.; Yan, H.; Marks, T. J.; van der Boom, M. E.; Facchetti, A. *J. Am. Chem. Soc.* **2010**, *132*, 12528–12530. (b) de Ruiter, G.; Motiei, L.; Choudhury, J.; Oded, N.; van der Boom, M. E. *Angew. Chem., Int. Ed.* **2010**, *49*, 4780–4783.

(13) (a) DiBenedetto, S. A.; Facchetti, A.; Ratner, M. A.; Marks, T. J. *Adv. Mater.* **2009**, *21*, 1407. (b) Zhao, Y.-G.; Chang, S.; Wu, A.; Lu, H.-L.; Ho, S. T.; van der Boom, M. E.; Marks, T. J. *Opt. Eng.* **2003**, *42*, 298.

(14) Altman, M.; Shukla, A. D.; Zubkov, T.; Evmenenko, G.; Dutta, P.; van der Boom, M. E. *J. Am. Chem. Soc.* **2006**, *128*, 7374.

(15) Altman, M.; Rachamim, M.; Ichiki, R.; Iron, M. A.; Evmenenko, G.; Dutta, P.; van der Boom, M. E. *Chem.−Eur. J.* **2010**, *16*, 6744.

(16) Altman, M.; Zenkina, O. V.; Ichiki, T.; Iron, M. A.; Evmenenko, G.; Dutta, P.; van der Boom, M. E. *Chem. Mater.* **2009**, *21*, 4676.

(17) Altman, M.; Zenkina, O.; Evmenenko, G.; Dutta, P.; van der Boom, M. E. *J. Am. Chem. Soc.* **2008**, *130*, 5040.

(18) Palomaki, P. K. B.; Dinolfo, P. H. *Langmuir* **2010**, *26*, 9677.

(19) (a) Zheng, Y.-R.; Stang, P. J. *J. Am. Chem. Soc.* **2009**, *131*, 3487. (b) Northrop, B. H.; Zheng, Y.-R.; Chi, K.-W.; Stang, P. J. *Acc. Chem. Res.* **2009**, *42*, 1554. (c) Stone, M. T.; Moore, J. S. *J. Am. Chem. Soc.* **2005**, *127*, 5928. (d) Seidel, S. R.; Stang, P. J. *Acc. Chem. Res.* **2002**, *35*, 972. (e) Leininger, S.; Olenyuk, B.; Stang, P. J. *Chem. Rev.* **2000**, *100*, 853. (f) Drain, C. M.; Lehn, J. M. *J. Chem. Soc., Chem. Commun.* **1994**, 2313.

(20) Stewart, J. J. P. *J. Mol. Model.* **2007**, *13*, 1173.

(21) (a) Motiei, L.; Lahav, M.; Gulino, A.; Iron, M. A.; van der Boom, M. E. *J. Phys. Chem. B* **2010**, DOI: 10.1021/jp910898f. (b) Motiei, L.; Lahav, M.; Freeman, D.; van der Boom, M. E. *J. Am. Chem. Soc.* **2009**, *131*, 3468. (c) Motiei, L.; Altman, M.; Gupta, T.; Lupo, F.; Gulino, A.; Evmenenko, G.; Dutta, P.; van der Boom, M. E. *J. Am. Chem. Soc.* **2008**, *130*, 8913.

(22) For a communication on linear vs exponential growth of metal−organic assemblies including chromophore **1**, see: Choudhury, J.; Kaminker, R.; Motiei, L.; de Ruiter, G.; Morozov, M.; Lupo, F.; Gulino, A.; van der Boom, *J. Am. Chem. Soc.* **2010**, *132*, 9295. Please note that a structurally different template layer was used to construct the assemblies.

Scheme 1. Molecular Structures of Chromophores **1** and **2**[22,23]

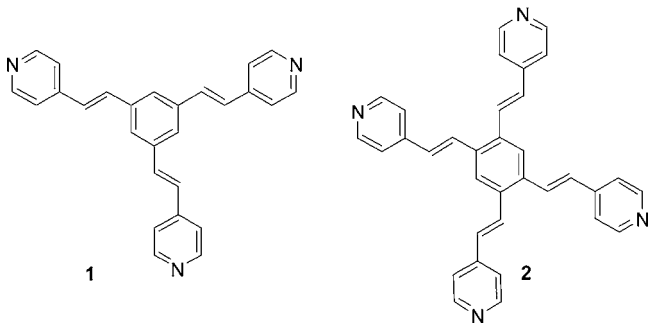

+ palladium dichloride) was observed, while the chromophore−palladium ratios imply the formation of fully cross-linked structures.

Results and Discussion

Chromophores **1** and **2** were selected for this study because of their branched structures that could allow for the formation of extended networks with $PdCl_2$ (Scheme 1). The generation of the MONs is based on the square-planar coordination chemistry of Pd(II) and the *trans* positioning of the pyridine-based ligands. This metal−ligand combination has been utilized by Lehn, Stang, Moore, and others to generate and study the formation and physicochemical properties of various well-defined structures in solution.[19] It has also been shown to be a powerful directing structural unit in solid-state materials.[14−17] In this study, the MONs were built on pyridine-terminated template layers by alternate immersion of the substrates in solutions containing either the palladium precursor ($PdCl_2(PhCN)_2$) or the chromophore (**1** or **2**).

A series of possible ring structures with four to seven chromophore **1**/$PdCl_2$ units were evaluated computationally. In each case, a closed ring-structure was found where the palladium complexes, with the exception of the smallest ring, were all *trans* coordinated; in the smallest ring, one of the four palladium atoms had a *cis* coordination, likely due to ring strain. The ring formation energy per chromophore is similar for the pentamer, hexamer, and heptamer, while for the tetramer, it is higher by ∼4 kcal/mol. One structure—the hexamer—is the most interesting since it formed a regular, planar, hexagonal structure with C_6 symmetry induced by the intrinsic geometric nature of the chromophore (Figure 1, left). The C_{6h} symmetry is broken by the rotation of the Cl−Pd−Cl axis relative to the pyridine rings. This rotation has been observed in related complexes[16] and experimentally in a model complex (**3**) presented hereinafter. This hexameric structure is ideally suited to form regular two-dimensional (2D) honeycomb structures. These extended 2D networks have also been optimized (Figure 2, left). The four-armed chromophore **2** is well-suited to form a tetrameric parallelogram-shaped structure that can also be used as building blocks for extended networks (Figure 1, right and Figure 2, right). Thus, these systems are indeed suitable candidates for constructing extended supramolecular networks. Honeycomb and related structures have been observed,[24] for example, by the formation of hydrogen-bonding networks for both trimesic acid and perylene diimide/melamine.[25]

Template layers (**T1**,**T2**) are prepared by immersing chlorobenzyl-functionalized glass and silicon substrates[26] into dry toluene and toluene/acetonitrile (1:1 v/v) solutions of chromophores **1** or **2**, respectively, at elevated temperatures for 3 days under N_2 in glass pressure tubes. The resulting films are robust and strongly adhere to the substrate surfaces (Scheme S1, Supporting Information). DFT optimized molecular structures of **T1** and **T2** are shown in Figure 3.

High-resolution XPS measurements of the functionalized silicon substrates reveal the formation of pyridinium salts by quarternization of only one pyridyl moiety of chromophores **1** or **2**. The pyridinium and pyridyl N 1s signals were observed for both templates at 402.2 and 399.8 eV, respectively,[27−29] with elemental ratios N^+/N of 0.5 (**1**) and 0.3 (**2**) (Figure 4A,B). This remarkable selectivity is most probably the result of the relatively rigid and planar molecular structures. It is known that variations of porphyrin ring substituents and other chromophores allow control over the molecular orientation on the surface and the degree of quarternization.[27,30] The thickness of the films was obtained by ellipsometry (**1**: 1.7 nm, **2**: 1.9 nm) and by

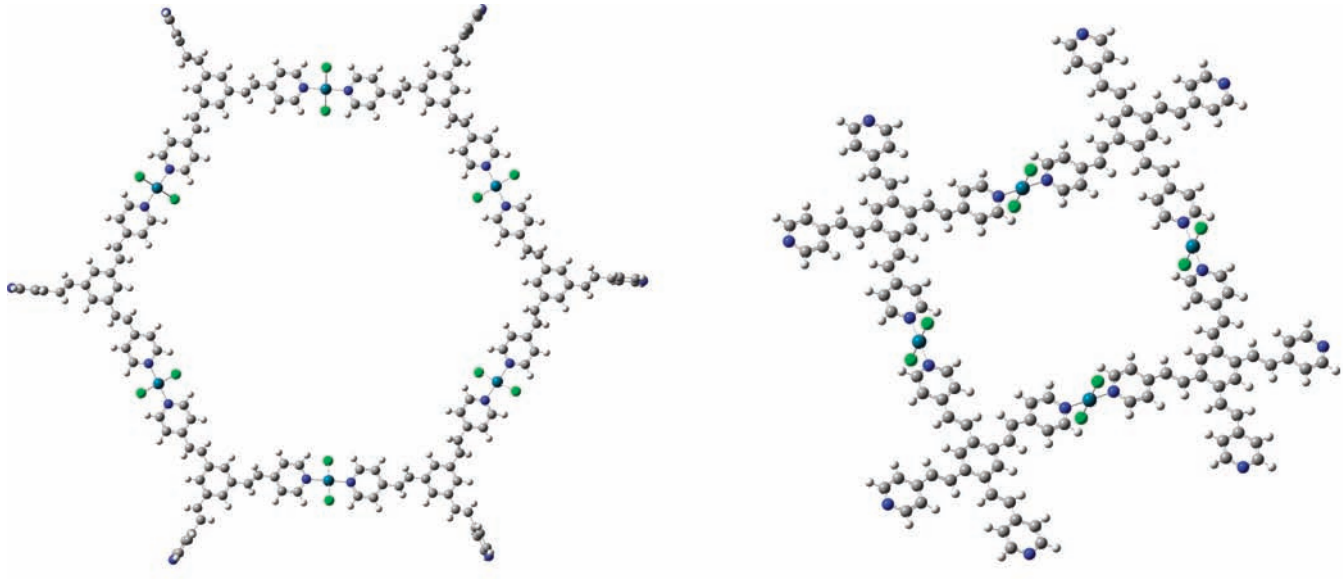

Figure 1. Computationally (PM6) optimized structures. (Left) Cyclic hexamer of chromophore **1** and $PdCl_2$. (Right) Cyclic tetrameric structure of chromophore **2** and $PdCl_2$.

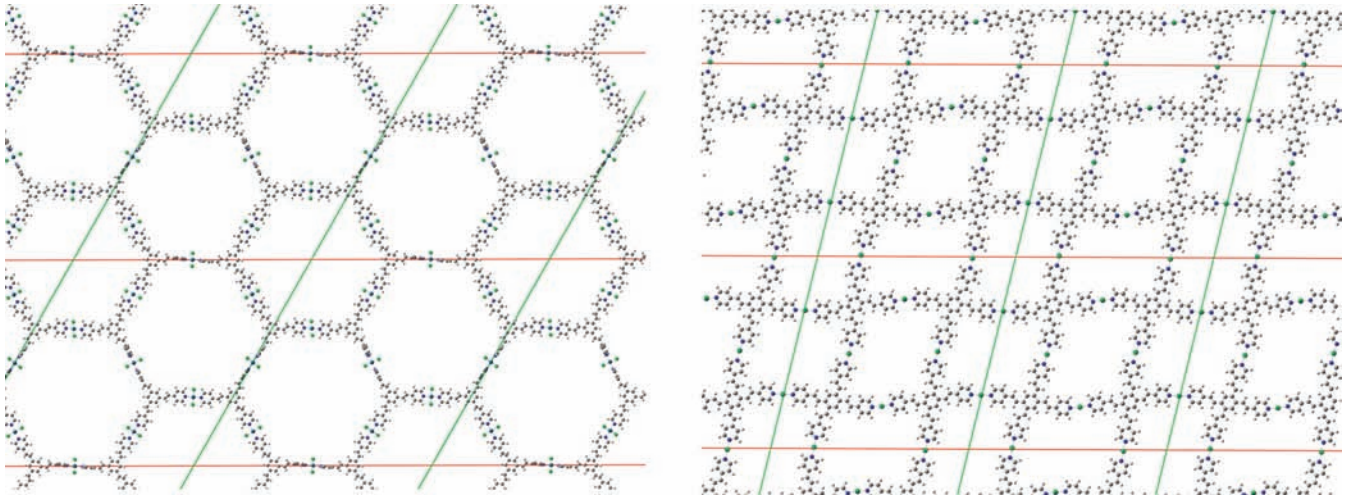

Figure 2. Computationally predicted extended networks formed from chromophores **1** (left) or **2** (right) with $PdCl_2$. The cross-ring Pd−Pd distances are 3.5 nm (**1**) and 1.7 and 2.2 nm (**2**).

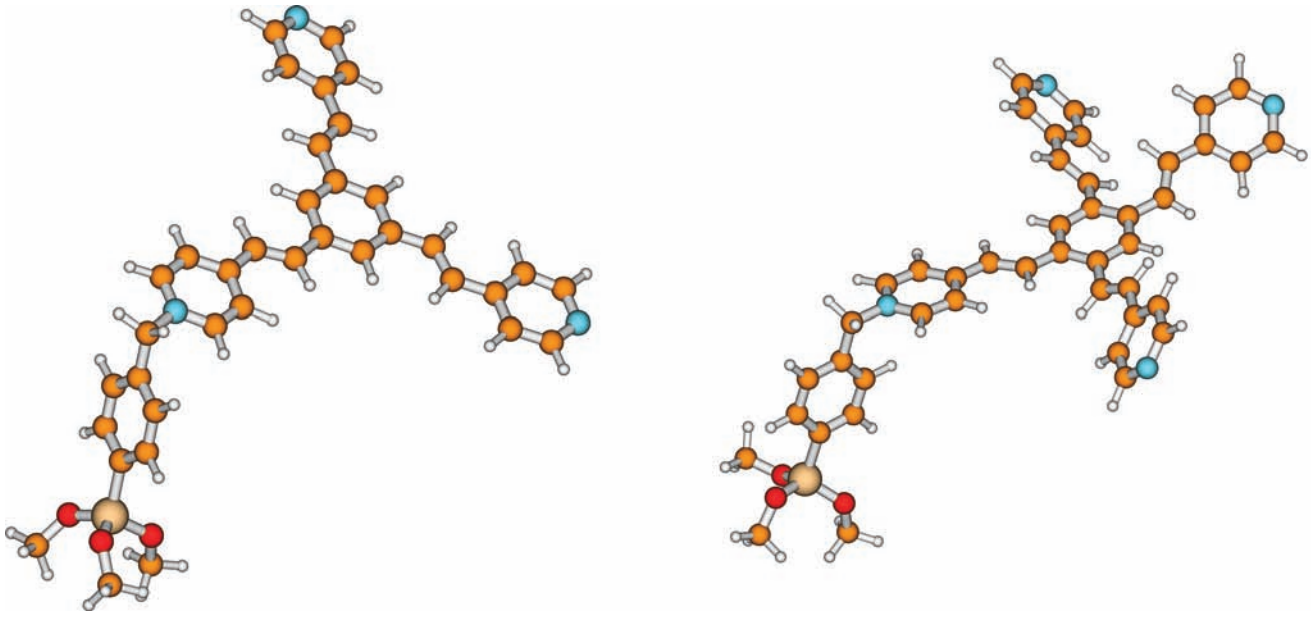

Figure 3. DFT optimized molecular structures of the pyridinium salts of chromophores **1** and **2** as calculated at the M06-L/pc-1/DFBS level of theory. A $(MeO)_3Si$ unit was used in these models of template layers **T1** and **T2**. Atomic color scheme: O, red; C, orange; N, light blue, H, white. The bend angles (defined as the angle between the Ph(C)−CH_2−PyN) are ∼112°. Assuming that the SiPh unit is perpendicular to the surface, then the systems are tilted ∼22° to the surface. The estimated thicknesses are 1.4 nm (**T1**) and 1.5 nm (**T2**).

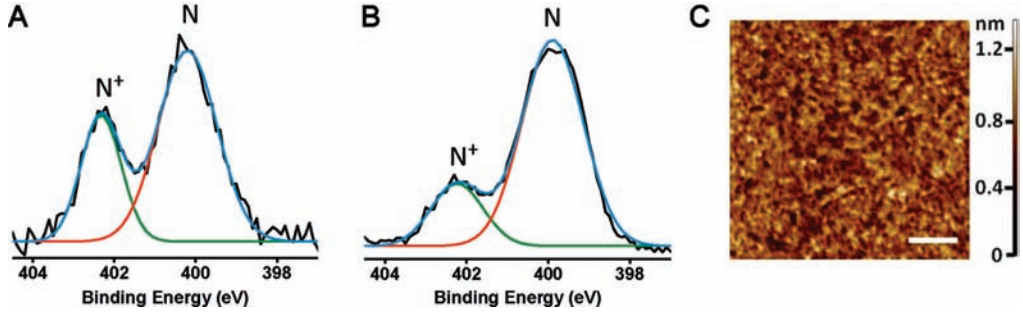

Figure 4. (A and B) XPS data of template layers **T1** and **T2** (Scheme S1, Supporting Information), respectively. The high-resolution XPS spectra shows the two N 1s signals. The black line represents the experimental data, while the blue line is the accumulative calculated spectrum for both nitrogen signals using a Gaussian fit. On the basis of the deconvolution of the spectrum, the red and green traces represent the unreacted pyridine group (N) and the pyridinium unit (N^+), respectively. (C) AFM data of the template layer **T1** on a silicon substrate. The representative tapping mode AFM image is for a 500 nm × 500 nm scan area with a R_{rms} of ∼0.2 nm. The scale bar represents 100 nm. AFM data for template layer **T2** are included in the SI (Figure S3, Supporting Information).

Table 1. Elemental Pd/N Ratios Derived from Angle-Resolved XPS Measurements at Various Take-off Angles for **MON1** and **MON2**

	5°	15°	30°	45°	80°
MON1	0.49	0.57	0.57	0.51	0.54
MON2	0.46	0.44	0.47	0.47	0.44

synchrotron XRR measurements (**1**: 1.9 nm, **2**: 2.1 nm) (Figure S1, Supporting Information). These values are in good agreement with the molecular dimensions (Figure 3). The chlorobenzyl-terminated layer is ~0.8 nm thick, and the calculated length of chromophores **1** and **2** are ~1.3 nm and ~1.6 nm, respectively. The films are densely packed with XRR-derived chromophore densities of ~3 molecules/nm^2, whereas the molecular density for the coupling layer is ~3.8 molecules/nm^2. The estimated yield of the quaternization process is high (~79%). A quantitative reaction is not expected because of the relatively large molecular dimensions of the surface-bound chromophores versus the smaller chlorobenzyl units. A template layer with a high density of coordination sites is necessary to prevent dendritic growth.[31] Tapping mode AFM measurements showed homogenously covered silicon surfaces with a root-mean-square roughness (R_{rms}) of ~0.2 nm for 500 nm × 500 nm scan areas (Figures 4C, S2, and S3 (Supporting Information)), which is comparable to the low XRR-derived roughness of 0.5 nm (**1**) and 0.3 nm (**2**).

Functionalized silicon and glass substrates (with the films of the pyridinium salts **T1** or **T2**) were fully immersed in a THF solution of $PdCl_2(PhCN)_2$ (1.0 mM) for 15 min at room temperature. Subsequently, the samples were immersed in a THF solution containing chromophore **1** or **2** (1.0 mM) for 15 min. The samples were washed and sonicated in organic solvents and dried under a stream of N_2 between each treatment. This two-step assembly process was repeated five times, conveniently in air, to generate the chromophore-terminated MONs (**MON1** and **MON2**).

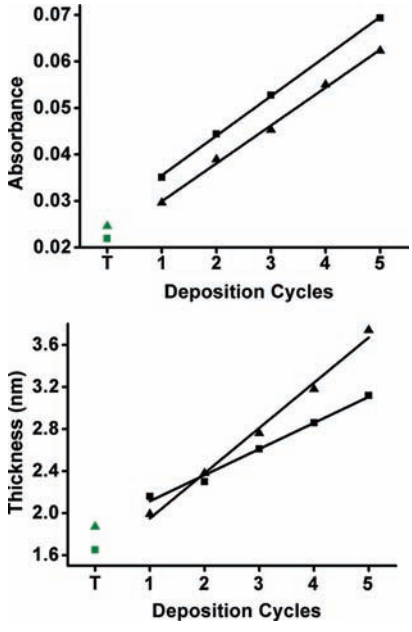

Figure 5. UV/vis maximum absorption (left) and ellipsometry-derived thickness (right) vs the number of deposition cycles for **MON1** (335 nm, ■) and **MON2** (353 nm, ▲). All lines are linear fits with $R^2 = 0.99$. The data of the template layers (**T**: **1**, ■ (green), and **2**, ▲ (green)) were excluded from these fits. The UV/vis spectra are shown in Figure S5 (Supporting Information).

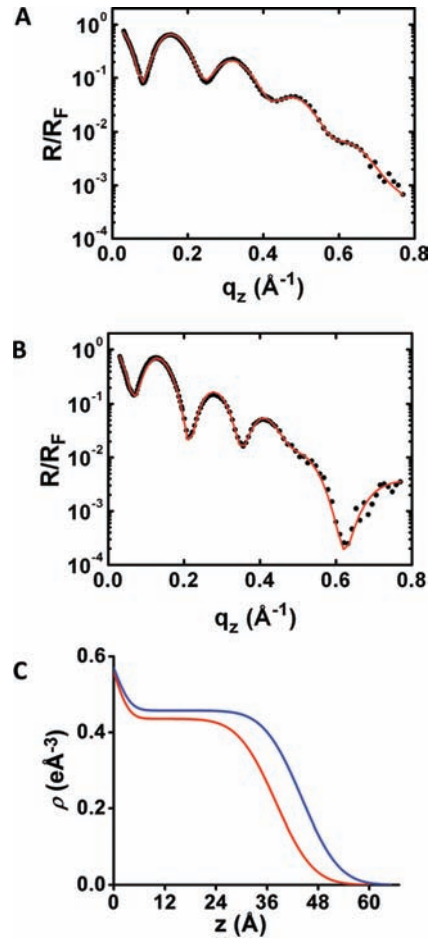

Figure 6. Representative XRR spectra of **MON1** (A) and **MON2** (B). The red traces are fits of the experimental data (black dots).[33] Figure C shows the electron density profiles of **MON1** (red trace) and **MON2** (blue trace) as functions of the distance from the substrate surface.

The generation of the MONs was revealed by high-resolution angle-resolved XPS (AR-XPS) measurements showing average elemental ratios of Pd/N of 0.54 (**MON1**) and 0.46 (**MON2**). Similar Pd/N values are obtained for takeoff angles in the range 5°−80° (Table 1) and indicate the formation of homogeneous assemblies. The experimental data is in very good agreement with the expected Pd/N value of 0.50 and demonstrate that the MON formation is based on nearly quantitative pyridine−metal−pyridine coordination.

For both assemblies, the uniform growth is evident from the linear increase of the UV/vis absorption and ellipsometrically determined film thickness with each deposition cycle. The positions of the absorption maxima remain nearly constant at $\lambda_{max} \approx 335$ nm (**1**) and 353 nm (**2**), which demonstrates that these two assemblies do not undergo significant structural or conjugational changes with MON expansion. The thicknesses of **MON1** and **MON2** are 3.1 and 3.7 nm, respectively, after five deposition cycles (Figure 5). Interestingly, the average increase in the thickness of the MONs with each deposition cycle seems low (**MON1**: 0.3 nm and **MON2**: 0.4 nm), indicating that the overall orientation of the chromophores is almost parallel to the substrate surface. Such a growth model is to some extent supported by the relatively large XRR-derived average footprint of 1.1 nm^2 and 1.2 nm^2 for each subunit **1**·1^1/$_2$PdCl$_2$ or **2**·2PdCl$_2$ of the assembly, respectively. The footprints based on the computational model above are 1.0 nm^2 and 1.6 nm^2, respectively, determined

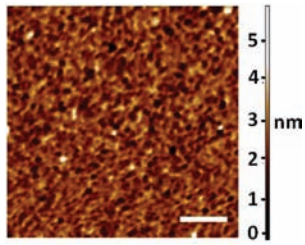

Figure 7. Representative tapping mode AFM image of **MON1** on a silicon substrate. The 500 nm × 500 nm scan area has an R_{rms} of ∼0.5 nm. The white scale bar represents 100 nm. The AFM image of **MON2** is shown in Figure S6 (Supporting Information).

from the area of the ring and the bending angle in the template layers of 22° (**T1**) and 23° (**T2**) (Figure 3). This is in reasonable agreement taking into consideration the experimental uncertainties and the coarse models used to fit the data. A fully branched polymeric structure without (significant) cross-linking between individual sheets seems to be a realistic possibility. The footprints would indicate that the MONs are porous. This can be demonstrated by an electrochemical (cyclic voltammetry) experiment where oxidation/reduction is observed for 2,6-di-*tert*-butylcyclohexa-2,5-diene-1,4-dione in an acetonitrile solution with indium−tin-oxide (ITO) electrodes, both bare and coated with **MON1** (Figure S4, Supporting Information). Apparently, the redox probe can interact with the functionalized electrode surface.[32]

The thicknesses obtained by XRR (Figure 6) and AR-XPS (**MON1**: 3.9 and 3.4 nm; and **MON2**: 4.4 and 4.0 nm) for the same assemblies are somewhat higher than those derived by ellipsometry, but the thickness of **MON2** is always larger than for **MON1**. The 0.5 nm difference between the thicknesses of the two assemblies is likely due to the dimensions of the chromophores and is an example of how molecular structures can be expressed in the properties of much larger assemblies. The XRR-derived roughness for both structures is only 0.7 nm, which is comparable with the XRR-derived values for the template layers and provides additional evidence for the presence of an organized assembly. Moreover, no distinctive electron density variations were observed (Figure 6C). The uniform electron density profiles corroborate very well with the XPS, UV/vis, and ellipsometry data.

A representative semicontact AFM image of **MON1** after five deposition cycles is shown in Figure 7. The roughnesses of **MON1** and **MON2** are similar to the XRR data (R_{rms} = 0.5 nm for 500 nm × 500 nm scan areas). Both the MONs and the template layers have to some extent similar homogeneous,

Scheme 2. Formation of a Model of the **1**-Based MON

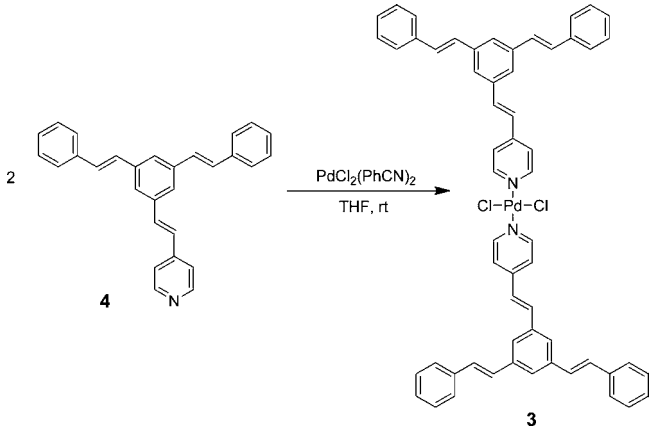

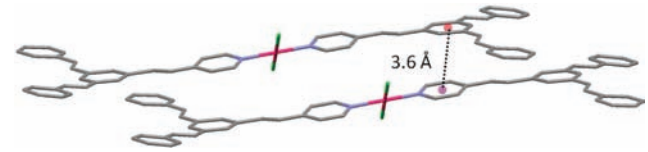

Figure 8. The X-ray-determined packing structure for complex **3**, indicating $\pi-\pi$ interactions (dashed lines) between the pyridine units (purple) and the central aromatic rings (orange). Hydrogen atoms and solvent molecules are excluded for clarity. Colors: gray - carbon, blue - nitrogen, pink - palladium, green - chloride. See the Experimental Section and the Supporting Information for details (Figure S7).

grainy surfaces. Some gaps, however, are observable in the MONs with diameters of ∼15 nm and depths of ∼1.5 nm, which might reflect defects in the underlying template layers. Such features are not uncommon.[16]

To provide additional support for our observations, a model complex (**3**) was prepared in solution. Complex **3** was formed quantitatively by the room temperature reaction between ligand **4** and $PdCl_2(PhCN)_2$ in THF in a 2:1 ratio. Ligand **4** is structurally related to chromophore **1** but contains only one pyridine unit (Scheme 2 and Figure 8).

This new compound was structurally characterized by ^1H and $^{13}C\{^1H\}$ NMR spectroscopy, elemental analysis, powder XPS, and single-crystal X-ray diffraction. The ^1H NMR data shows that the pyridine protons adjacent to the N atom are shifted downfield by 0.2 ppm, indicative of metal coordination to the pyridine moiety. Powder XPS measurements revealed a Pd/N ratio of 0.49, demonstrating that our MONs can be accurately validated by this method. Furthermore, the crystal structure analysis of complex **3** unambiguously reveals the square-planar ligand arrangement around the d^8 metal center with the two pyridyl units in a mutually *trans* configuration. In fact, the two ligands (**4**) coordinated to the metal center are essentially aligned in one plane and are tilted by 44.6(3)° to the chloride ligands, in good agreement with the 41.7° in the calculated structure (Figure 1). These facts lend support to our proposed stepwise-grown structures. The distance of 3.6 Å between the pyridyl ring of one complex and the central benzene ring of the adjacent complex is typical of $\pi-\pi$ stacking. The intermolecular distance between the planes of two pyridyl rings is 4.2 Å. The electron density of the crystal structure is 0.38 e·Å^{-3}, which is lower than the XRR-derived electron density for **MON1** (0.43−0.45 e·Å^{-3}). The crystal packing of complex **3** is obviously different than the structure of the MONs as it contains fewer $PdCl_2$ units/

(23) (a) Kaminker, R.; Lahav, M.; Motiei, L.; Vartanian, M.; Popovitz-Biro, R.; Iron, M. A.; van der Boom, M. E. *Angew. Chem., Int. Ed.* **2010**, *49*, 1218. (b) Amoroso, A. J.; Cargill Thompson, A. M. W.; Maher, J. P.; McCleverty, J. A.; Ward, M. D. *Inorg. Chem.* **1995**, *34*, 4828.

(24) (a) Maruccio, G.; Arima, V.; Cingolani, R.; Liantonio, R.; Pilati, T.; Rinaldi, R.; Metrangolo, P. *CrystEngComm* **2009**, *11*, 510. (b) Barth, J. V. *Surf. Sci.* **2009**, *603*, 1533. (c) Coronado, E.; Galan-Mascaros, J. R.; Gavina, P.; Marti-Gastaldo, C.; Romero, F. M.; Tatay, S. *Inorg. Chem.* **2008**, *47*, 5197. (d) Dmitriev, A.; Lin, N.; Weckesser, J.; Barth, J. V.; Kern, K. *J. Phys. Chem. B* **2002**, *106*, 6907. (e) Sharma, C. V. K.; Clearfield, A. *J. Am. Chem. Soc.* **2000**, *122*, 4394. (f) Choi, H. J.; Lee, T. S.; Suh, M. P. *Angew. Chem., Int. Ed.* **1999**, *38*, 1405. (g) Stang, P. J.; Fan, J.; Olenyuk, B. *Chem. Commun.* **1997**, 1453. (h) Ozin, G. A. *Acc. Chem. Res.* **1997**, *30*, 17.

(25) (a) Theobald, J. A.; Oxtoby, N. S.; Phillips, M. A.; Champness, N. R.; Beton, P. H. *Nature* **2003**, *424*, 1029. (b) Barth, J. V.; Costantini, G.; Kern, K. *Nature* **2005**, *437*, 671.

chromophore. Nevertheless, these results give a clear indication that the molecular density of the surface-bound network is high.

Summary and Conclusions

The multibranching chromophores **1** and **2** are both excellent materials for the assembly of uniform MONs in a stepwise approach. Formation of supramolecular architectures often involves a fine balance between rigidity and flexibility of the individual components.[34] Despite the relatively rigid structures of these two compounds, the formation of fully coordinated networks is still possible. In fact, these chromophores have optimal geometries well suited for network formation, as suggested by computation and supported by experiments. AR-XPS measurements give Pd/N ratios appropriate for such a system. However, the modeled structures do not necessarily have to resemble the experimental ones. For instance, we cannot exclude the formation of intertwined rings or other defects. The optical data indicates that network formation does not extend the conjugation inherent to the constituent chromophore units. This basic study on the controlled formation and structure of metal−organic materials is not an assessment of their potential properties. Functionality can be rationally designed on the basis of an understanding of the structures involved, as we have demonstrated recently with our self-propagating materials.[12] Future studies will include the use of three-dimensional structured organic chromophores and the here presented MONs as interlayers for inverted bulk-heterojunction solar cells.

Experimental Section

Materials and Methods. Chemicals were purchased from Sigma-Aldrich and Acros Organics. Solvents were reagent grade (AR) from either Bio-Lab (Jerusalem) or Frutarom (Haifa). Pentane and toluene were dried using an M. Braun solvent purification system and degassed before being introduced into an M. Braun glovebox. Acetonitrile (anhydrous, 99.98%) was purchased from Aldrich. Compounds **1**, **2**, **4**, $PdCl_2(PhCN)_2$, and the chlorobenzyl-terminated layer were prepared as reported.[23,27,35] Reaction tubes were washed with deionized (DI) water followed by acetone and then oven-dried overnight at 130 °C. All glassware and Teflon holders for film formation were cleaned by immersion in a piranha solution (7:3 v/v H_2SO_4/30% H_2O_2) for 10 min and then DI water. *Caution: piranha is an extremely dangerous oxidizing agent and should be handled with care using appropriate personal protection*. Single-crystal silicon ⟨100⟩ substrates, purchased from Wafernet (San Jose, CA), were cleaned by sonication for 8 min sequentially in *n*-hexane, acetone, and ethanol and dried under a stream of N_2. Then the slides were treated with a UVOCS cleaning system (Montgomery, PA), washed with isopropanol, dried under a stream of N_2, and heated overnight at 130 °C in an oven. Glass slides having a size 2.5 cm × 0.8 cm × 0.1 cm (Chase Scientific Glass, Rockwood, TN) were rinsed with DI water and cleaned by immersion in a piranha solution for 1 h. The substrates were then rinsed with DI water followed by the RCA cleaning protocol: a 1:5:1 (v/v) solution of $NH_3 \cdot H_2O/H_2O/30\%$ H_2O_2 at room temperature for 1 h. The substrates were subsequently washed with DI water and isopropanol, dried under an N_2 stream, and heated overnight at 130 °C in an oven.

The ^1H and $^{13}C\{^1H\}$ NMR spectra were obtained in $CDCl_3$ using a Bruker AMX 400 NMR spectrometer. All chemical shifts (δ) are reported in ppm relative to tetramethylsilane, and the coupling constants (J) are in Hz. Elemental Analyses were performed by H. Kolbe, Mikroanalytisches Laboratorium, Mülheim an der Ruhr, Germany. UV/vis spectra were recorded on glass slides with a Cary 100 spectrophotometer with the double beam mode. Atomic force microscopy (AFM) images were recorded using a Solver P47 (NT-MDT, Russia) operated in the semicontact/tapping scanning mode. Silicon cantilevers (∼100 μm) were used with a resonant frequency of 70−90 kHz. The roughness values, R_{rms}, were obtained from 500 nm × 500 nm images using silicon substrates. Several areas with different scanning size were analyzed (3 μm and 500 nm). Film thicknesses were estimated using a J.A. Woollam (Lincoln, NB) model M-2000 V variable angle spectroscopic ellipsometer with VASE32 software. Measurements were performed on silicon for each 5° in a range of 50°−80° over wavelengths of 399−1000 nm. Parameters A, B, and C were 1.45, 0.01, and 0.00, respectively, with MSE < 10 for a Cauchy model. The SiO_2 layer was calibrated to be 17 Å.

Angle resolved X-ray photoelectron spectroscopy (AR-XPS) measurements were performed at the University of Catania, Italy. Films on silicon and quartz substrates were measured at five different takeoff angles relative to the surface plane (5°, 15°, 30°, 45°, 80°) with a PHI 5600 MultiTechnique System (base pressure of the main chamber 2×10^{-10} Torr). The acceptance angle of the analyzer and the precision of the sample holder concerning the takeoff angle are ±3° and ±1°, respectively. Samples were mounted on Mo stubs and were excited with Al Kα radiation. The silicon slides were radiated using a monochromator. High-resolution spectra of C(1s), O(1s), Si(2p), N(1s), Pd(3d), and Cl(2p) were collected with 5.85 eV pass energy and resolutions of better than 0.3 and 0.5 eV for silicon and quartz, respectively.[36] The structure due to satellite $K\alpha_2$ radiation was subtracted from the spectra of quartz slides, radiated with the unmonochromatized source, before data processing. The XPS peak intensities were obtained after Shirley background removal, and the curves were fit to Gaussians. The C(1s) line at 285.0 eV was used for calibration.

X-ray reflectivity (XRR) measurements were performed at beamline X6B of the National Synchotron Light Source, Brookhaven (U.S.A.) using a four-circle Huber diffractometer in the specular reflection mode (i.e., incident angle $\hat{I}$ was equal to the exit angle). X-rays with an energy of $E = 10.0$ keV ($\lambda = 1.240$ Å) were used. The beam size was 0.40 mm vertically and 1.2 mm horizontally. The samples were held under a helium

(26) Li, D. Q.; Ratner, M. A.; Marks, T. J.; Zhang, C.; Yang, J.; Wong, G. K. *J. Am. Chem. Soc.* **1990**, *112*, 7389.
(27) (a) Facchetti, A.; Beverina, L.; van der Boom, M. E.; Dutta, P.; Evmenenko, G.; Shukla, A. D.; Stern, C. E.; Pagani, G. A.; Marks, T. J. *J. Am. Chem. Soc.* **2006**, *128*, 2142. (b) Yerushalmi, R.; Scherz, A.; van der Boom, M. E. *J. Am. Chem. Soc.* **2004**, *126*, 2700.
(28) Shukla, A. D.; Strawser, D.; Lucassen, A. C. B.; Freeman, D.; Cohen, H.; Jose, D. A.; Das, A.; Evmenenko, G.; Dutta, P.; van der Boom, M. E. *J. Phys. Chem. B* **2004**, *108*, 17505.
(29) Briggs, D.; Seah, M. P. *Practical Surfaces Analysis*, 2nd ed.; Wiley-VCH: Weinheim, Germany, 1995; Vol. 1.
(30) Zong, H.; Sun, P.; Mirkin, C. A.; Barrett, A. G. M.; Hoffman, B. M. *J. Phys. Chem. B* **2009**, *113*, 14892.
(31) (a) Wanunu, M.; Vaskevich, A.; Shanzer, A.; Rubinstein, I. *J. Am. Chem. Soc.* **2006**, *128*, 8341. (b) Wanunu, M.; Vaskevich, A.; Cohen, S. R.; Cohen, H.; Arad-Yellin, R.; Shanzer, A.; Rubinstein, I. *J. Am. Chem. Soc.* **2005**, *127*, 17877.
(32) (a) Williams, M. E.; Benkstein, K. D.; Abel, C.; Dinolfo, P. H.; Hupp, J. T. *Proc. Natl. Acad. Sci. U.S.A.* **2002**, *99*, 5177. (b) Dinolfo, P. H.; Hupp, J. T. *Chem. Mater.* **2001**, *13*, 3113. (c) Lee, J.-Y.; Park, S.-M. *J. Phys. Chem. B* **1998**, *102*, 9940. (d) Motesharei, K.; Ghadiri, M. R. *J. Am. Chem. Soc.* **1997**, *119*, 11306.
(33) Evmenenko, G.; van der Boom, M. E.; Dugan, S. W.; Kmetko, J.; Marks, T. J.; Dutta, P. *J. Chem. Phys.* **2001**, *115*, 6722.
(34) (a) Beverina, L. *ChemPhysChem* **2010**, *11*, 2075. (b) Lehn, J.-M. *Chem. Soc. Rev.* **2007**, *36*, 151.
(35) (a) Reddy, L. S.; Bhogala, B. R.; Nangia, A. *CrystEngComm* **2005**, *7*, 206. (b) Wang, L.; Tao, X.-T.; Yang, J.-X.; Yu, W.-T.; Ren, Y.; Xin, Q.; Liu, Z.; Jiang, M.-H. *J. Solid State Chem.* **2004**, *177*, 4293. (c) Sun, S. S.; Anspach, J. A.; Lees, A. J. *Inorg. Chim. Acta* **2003**, *351*, 363. (d) Anderson, G. K.; Lin, M. *Inorg. Synth.* **1990**, *28*, 60.
(36) (a) Gulino, A.; Lupo, F.; Fragalà, M. E.; Schiavo, S. L. *J. Phys. Chem. C* **2009**, *19*, 3507. (b) Cerofolini, G. F.; Galati, C.; Renna, L. *Surf. Interface Anal.* **2003**, *35*, 968.

atmosphere during the measurements to reduce radiation damage and the background scattering from the ambient gas. The off-specular background was measured and subtracted from the specular counts.

Template Layer Formation (T1, T2) with Chromophores 1 or 2. Chromophore **1** (5.8 mg, 0.015 mmol) or **2** (7.4 mg, 0.015 mmol) was dissolved in dry toluene (30 mL) by heating to 40 °C, and in dry toluene/acetonitrile (1:1, v/v) (30 mL) at 80 °C, respectively, for 30 min. These 0.5 mM solutions were degassed under argon and loaded together with chlorobenzyl-functionalized glass and silicon substrates in glass pressure tubes under N_2. The sealed tubes were heated at 100 °C (**1**) and 87 °C (**2**) for 72 h with exclusion of light. Subsequently, the slides were sonicated consecutively in toluene, CH_2Cl_2, isopropanol for 6 min, cleaned with Kimwipes, wetted with ethanol, sonicated again, and dried under a stream of N_2 (Scheme S1, Supporting Information).

Stepwise Formation of the Coordination-Based Networks (MON1 and MON2). The glass and silicon substrates, functionalized with a **1**- or **2**-based template layer, were rinsed with THF and then immersed for 15 min in a THF solution (20 mL) of $PdCl_2(PhCN)_2$ (7.7 mg, 1.0 mM) at room temperature. The samples were then sonicated in THF (×2) and in acetone (×1) for 3 min each. The substrates were rinsed with THF and then immersed in 1.0 mM chromophore solutions (**1**: 7.7 mg in 20 mL THF or **2**: 14.7 mg in 30 mL THF/DMF = 8:2, v/v) for 15 min at room temperature. The samples were then sonicated in THF (×2) and in acetone (×1) for 3 min each. Five chromophore layers were grown using this stepwise deposition procedure. The $PdCl_2(PhCN)_2$ and chromophore solutions remained clear during the multilayer formation. Similar results were obtained by reusing or discarding the solutions after each deposition step. The slides were rinsed with ethanol and dried under a stream of N_2.

Formation of Complex 3. A solution of ligand **4** (41 mg, 0.11 mmol) in THF (5 mL) was added slowly to a stirred solution of $PdCl_2(PhCN)_2$ (20 mg, 0.05 mmol) in THF (5 mL). The resulting yellow solution was dried under vacuum. The powder was then washed with pentane (×3) and dried again under vacuum to yield a yellow powder. X-ray quality crystals were obtained from a solution of toluene/CH_2Cl_2/THF (1:1:1, v/v/v) at room temperature. ^{1}H NMR ($CDCl_3$): δ 8.75 (d, PyrH, $^3J_{HH}$ = 6.7 Hz, $^4J_{HH}$ = 1.2 Hz), 7.66 (br, ArH), 7.58 (m, 6H, ArH), 7.41 (m, ArH), 7.31 (m, ArH), 7.28 (s, ArH), 7.23 (d, CH═CH, J_{HH} = 16.4 Hz) 7.16 (d, CH═CH, J_{HH} = 16.3 Hz), 7.10 (d, CH═CH, J_{HH} = 16.2 Hz). ^{13}C{^{1}H} NMR ($CDCl_3$): δ 152.65, 147.28 (C_q), 138.18 (C_q), 136.72 (C_q), 136.10 (C_q), 135.10, 129.64, 128.54, 127.75, 127.49, 126.40, 125.45, 124.42, 124.42, 121.75. UV/vis (THF) λ = 317 nm (ε = 5.2 × 10^4 M^{-1} cm^{-1}). Elemental Analysis (%) calcd. for $C_{58}H_{46}Cl_2N_2Pd$: C, 73.46; H, 4.89; found: C, 73.04; H, 5.11.

X-ray Analysis of Complex 3. *Crystal data*: $C_{61}H_{49}Cl_2N_2Pd$, prism, 0.12 × 0.07 × 0.04 mm^3, Monoclinic, *P*2/*c*, a = 17.8217(13) Å, b = 6.8370(5) Å, c = 26.0357(16) Å, β = 124.977(4)°, from 20 degrees of data, T = 100(2) K, V = 2599.4(3) Å^3, Z = 2, Fw = 987.34, D_c = 1.261 Mg·m^{-3}, μ = 0.499 mm^{-1}. *Data collection and processing*: Bruker Kappa ApexII CCD diffractometer, Mo Kα λ = 0.71073 Å, graphite monochromator, MiraCol optics, $-19 \le h \le 21$, $-6 \le k \le 8$, $-31 \le l \le 31$, $2\theta_{max}$ = 51.36°, frame scan width = 0.5°, scan speed 1.0° per 60 s, typical peak mosaicity 1.10°, 19665 reflections collected, 4928 independent reflections (R_{int} =0.055). The data were processed with Bruker Apex2. *Solution and refinement*: structure solved by direct methods with SHELXS-97.[37] Full matrix least-squares refinement based on F^2 with SHELXL-97,[37] 310 parameters with 0 restraints, final R_1 = 0.0589 (based on F^2) for data with $I > 2\sigma(I)$ and R_1 = 0.0985 on 4928 reflections, goodness-of-fit on F^2 = 1.033, largest electron density peak = 1.125 e·Å^{-3} and hole = 0.355 e·Å^{-3}.

Computational Details. All structures were optimized using the semiempircal method Parametric Method number 6 (PM6) using either Gaussian09[38] or MOPAC2007.[20,39] The systems under investigation are simply far too large to optimize with DFT. For example, the C_6-symmetric structure of the hexamer of **1** $PdC1_2$ was optimized at the PBE[40]/SDD(Pd)[41]+D95(H,C,N,Cl)[42]/DFBS[43] (density fitting basis sets, specifically the automatic DFBS generation algorithm implemented in Gaussian09) level of theory, but this required several weeks of wall time running on eight processors. The models of the template layer (**T1** and **T2**, Figure 3) were optimized at the M06-L/pc-1/DFBS level of theory, where M06-L[44] is Truhlar's local (i.e., nonhybrid) member of the M06 family of DFT functionals,[45] and pc-1 is Jensen's double-ζ polarization-consistent basis set.[46] All calculations were carried out using Gaussian09 except for PM6 calculation with periodic boundary conditions (PBC), which were performed with MOPAC2007.

Acknowledgment. This research was supported by The Helen and Martin Kimmel Center for Molecular Design, The Minerva Foundation, Mr. Martin Kushner Schnur, and the U.S. Department of Energy (Office of Basic Energy Sciences, Division of Materials Sciences and Engineering, Grant No. DE-FGO2-84ER45125). The X-ray reflectivity measurements were performed at Beamline X6B of the National Synchrotron Light Source. We thank Dr. Arkady Bitler (WIS) for his assistance with the AFM measurements. A.G. and I.F. thank the FIRB project ITALNANONET (RBPR05JH2P).

Supporting Information Available: Figures S1−S7, the complete reference 38, and the crystallographic information file (CIF) of complex **3**. This material is available free of charge via the Internet at http://pubs.acs.org.

JA105518N

(37) Sheldrick, G. M. *Acta Crystallogr.* **2008**, *A64*, 112–122.
(38) Frisch, M. J.; et al. *Gaussian09*, Revision A.02; Gaussian, Inc.: Wallingford CT, 2009.
(39) Stewart, J. J. P. *MOPAC2007*, Version 7.326L; Stewart Computational Chemistry: Colorado Springs, CO, U.S.A.; http://OpenMOPAC.net, 2007.
(40) (a) Perdew, J. P.; Burke, K.; Ernzerhof, M. *Phys. Rev. Lett.* **1996**, *77*, 3865. (b) Perdew, J. P.; Burke, K.; Ernzerhof, M. *Phys. Rev. Lett.* **1997**, *78*, 1396.
(41) Dolg, M. In *Modern Methods and Algorithms of Quantum Chemistry*; Grotendorst, J., Ed.; John von Neumann Institute for Computing: Jülich, 2000; Vol. 3, pp 507−540.
(42) Dunning, T. H., Jr.; Hay, P. J. In *Gaussian Basis Sets for Molecular Calculation*; Schaefer, H. F., III, Ed.; Plenum Press: New York, 1976; Vol. 3, pp 1−28.
(43) (a) Dunlap, B. I. *J. Chem. Phys.* **1983**, *78*, 3140. (b) Dunlap, B. I. *J. Mol. Struct. (THEOCHEM)* **2000**, *529*, 37.
(44) Zhao, Y.; Truhlar, D. G. *J. Chem. Phys.* **2006**, *125*, 194101.
(45) (a) Zhao, Y.; Truhlar, D. G. *Theor. Chem. Acc.* **2008**, *120*, 215. (b) Zhao, Y.; Truhlar, D. G. *Acc. Chem. Res.* **2008**, *41*, 157–167.
(46) (a) Jensen, F. *J. Chem. Phys.* **2001**, *115*, 9113. (b) Jensen, F. *J. Chem. Phys.* **2002**, *116*, 3502. (c) Jensen, F. *J. Chem. Phys.* **2002**, *116*, 7372. (d) Jensen, F. *J. Chem. Phys.* **2002**, *117*, 9234. (e) Jensen, F. *J. Chem. Phys.* **2003**, *118*, 2459. (f) Jensen, F.; Helgaker, T. *J. Chem. Phys.* **2004**, *121*, 3463.